



ELSEVIER

Contents lists available at ScienceDirect

## International Journal of Adhesion &amp; Adhesives

journal homepage: [www.elsevier.com/locate/ijadhadh](http://www.elsevier.com/locate/ijadhadh)

## Kinetic research on low-temperature cure of epoxy adhesive



Lanjuan Xia, Lu Zuo, Shangwen Zha, Shufang Jiang, Rong Guan, Deping Lu\*

Hubei Collaborative Innovation Center for Advanced Organic Chemical Materials, Ministry of Education Key Laboratory for the Synthesis and Application of Organic Functional Molecules, College of Chemistry and Chemical Engineering, Hubei University, Wuhan 430062, China

## ARTICLE INFO

## Article history:

Accepted 5 February 2014

Available online 17 February 2014

## Keywords:

Epoxy

DSC

Autocatalytic

Isoconversional method

Compensation parameters

Nonlinear regression

## ABSTRACT

Low-temperature cure of epoxy adhesives was investigated by means of differential scanning calorimetry analysis (DSC) on both isothermal and dynamic curing process and isothermal and dynamic curing phenomenological autocatalytic models were established. For dynamic curing section, an advanced isoconversional method was taken into account for computing the minimum apparent activation energy  $E_a$  value for each value of  $\alpha$  lying between 0.05 and 0.95 with a step of 0.01. The correlation of invariant apparent activation energy and pre-exponential factor was expressed by “compensation parameters” equation. The isothermal experimental results showed that curing at low-temperatures of 10–15 °C did take place but it was difficult to reach complete reaction over a reasonable experiment time period because the curing process was significantly decelerated owing to the effects of material vitrification and diffusion control in the late curing stages. In order to match the calculated and measured data better and describe the cure in the later stages of reaction, a heating rate-dependent pre-exponential factor and diffusion control were taken into account. The modified modeling with the heating rate-dependent pre-exponential factor and diffusion control agreed well with experimental data. Moreover, analysis of nonlinear regression was carried out on the isothermal modeling, results showed that the nonlinear least squares fitting had a satisfactory effect.

© 2014 Elsevier Ltd. All rights reserved.

## 1. Introduction

Epoxy resins are important thermosetting resins, as the matrix resin of adhesives which has been widely used in the field of mechanical engineering, transportation, chemical engineering, architecture, etc., owing to its better technology, mechanical and physical properties [1–4]. Additionally the composites have also been used for cryogenic applications [5]. Study on curing of matrix resin is one of the important issues. Kinetic model is commonly used, which established mathematical relationships between curing rate with temperature and curing degree from the computational standpoint [6]. The most straightforward way is to determine a kinetic triplet, that is  $A$ ,  $E_a$  and  $f(\alpha)$ .  $E_a$  is associated with the energy barrier,  $A$  with the frequency of vibrations of the activated complex [7], and  $f(\alpha)$  with the reaction mechanism [8].

Two main approaches used for cure kinetics can be divided into phenomenological and mechanistic modeling [9]. And the application of the phenomenological method mainly using semi-empirical model equation is more common, obtaining various parameters of

model equation through mathematical simulation [10–12]. The kinetics of curing epoxy resins has been widely studied by using isothermal or dynamic experiments with differential scanning calorimetry (DSC) [13]. A few reports have been reported on kinetic studies of high temperature curing of epoxy resins [14,15] but not much with low temperature curing [16]. Experience has told us that the mechanical properties are strongly dependent on the curing conditions [17], particularly long periods of low temperature are frequent in winter, the curing reaction may not be fully complete and the mechanical properties may change during use if the temperature is too low. Therefore, an understanding of the low-temperature curing mechanism is essential to control and optimize mechanical properties [18,19].

All experimental data have noise. The amount of noise can affect the choice of the kinetic analysis method. Since the differential isoconversional methods being more reliable for the treatment of thermoanalytical data [20–28] do not make use of any approximates on the temperature integral, they are more accurate than the integral methods. For differential isoconversional DSC data, it would be natural to use a differential method. According to Nicolas Sbirrazzuoli's literature [29], using compensation effect and the isoconversional method to compute a model-free estimate of the logarithm of the pre-exponential factor ( $\ln A$ ), ABS (Achar-Bridley-Sharp's) method and Tang method obtained the lowest

\* Corresponding author. Tel.: +860 27 5086 5386; fax: +860 27 8866 3043.

E-mail addresses: [xialanjuan@126.com](mailto:xialanjuan@126.com) (L. Xia), [zlumail@hubeu.edu.cn](mailto:zlumail@hubeu.edu.cn) (L. Zuo), [zsw4882535@163.com](mailto:zsw4882535@163.com) (S. Zha), [jiang.sf@qq.com](mailto:jiang.sf@qq.com) (S. Jiang), [rongguan@hubeu.edu.cn](mailto:rongguan@hubeu.edu.cn) (R. Guan), [ludeping13@126.com](mailto:ludeping13@126.com) (D. Lu).

errors and are more accurate than other methods. However, Tang method is an integral method and ABS method is a differential method, thus, we chose the ABS method to compute the  $\ln A$ . Moreover, the  $E_a$  value for each value of  $\alpha$  lying between 0.05 and 0.95 with a step of 0.01 was computed by the NLN Vyazovkin method [30–32].

This research work is now focused on two aspects: (I) looking for model parameters of a new system through the existing model, as providing a theoretical basis for the development of processing routes [33,34]. (II) Correcting the existing model or processing the new model to adapt to a new system. In this experiment, for the study on low-temperature curing of epoxy resin by DSC, a minimum curing temperature was 10 °C, used the aspect of (I). Assessing the validity of a kinetic model fitting by comparing the measured with calculated reaction profiles (either rates or extents of conversion, or both versus temperature) is required. Only by showing satisfactory matching can the parameters have some effectivity.

## 2. Experimental

### 2.1. Materials

The epoxy resin was diglycidyl ether of bisphenol A (DGEBA) type E-44 supplied by Yueyang Petrochemical and the curing agent was TU-DETA synthesized by our experiment. The structures of these chemicals were depicted in Table 1.

### 2.2. Methods

A differential scanning calorimeter (Shimadzu DSC-60, equipped with a liquid nitrogen cooling system and performed by TA analysis software for data acquisition) was used for dynamic and isothermal cure experiment and data analysis. The flux of nitrogen providing an insert atmosphere was set to 50 ml min<sup>-1</sup>.

The weight of each sample was measured prior to scanning by a ultramicro balance (XP6, Mettler Toledo). By the requirement of the Shimadzu instrument, the amount of sample was in the range of 5–10 mg. The samples were placed in an empty aluminum pan covered with a lid. An aluminum pan loading aluminum oxide as reference compound of the same type and size was used as a reference during every scan.

#### 2.2.1. Dynamic heating runs

Dynamic runs at constant heating rates were made in order to determine the total heats of reaction released during dynamic curing for uncured samples. Before testing, all uncured samples were deposited in refrigerator under –18 °C.

In order to determine the dosage of curing agent, the reactants E-44 and TU-DETA were mixed under –18 °C in a equivalent ratio of 2:1, 3:1, 4:1, 5:1, 6:1 and 7:1, respectively. These uncured samples of 5–10 mg were installed in aluminum pans and placed in the instrument furnace. After cooling to –50 °C rapidly, the

heat evolution was monitored from –50 °C to 250 °C using the heating rate of 10 °C min<sup>-1</sup>. After determining the optimum dosage to curing agent, dynamic scans were conducted in the temperature range of –50 °C to 250 °C at constant heating rates of 5, 10, 12.5, 15 and 20 °C min<sup>-1</sup>. By re-scanning the completely cured sample at 10 °C min<sup>-1</sup>, the corresponding glass transition temperature ( $T_g$ ) was obtained.

#### 2.2.2. Isothermal runs

Isothermal DSC scans were performed at temperatures ranging from 10 to 80 °C, where 10 °C was low temperature, 80 °C was high temperature below  $T_g$  in this experiment. This range was chosen in accordance with the planned architecture application. The furnace was first heated up to a desired fixed temperature at the heating rate of with 10 °C min<sup>-1</sup> and kept for a certain period of time. When the system reached the equilibrium state, the sample was quickly set on the calorimetric detector plate. The reaction was considered to be complete until the heat flow curve approached a plateau.

In this experiment, the sample used was fresh and uncured. The curing heat of each sample at its corresponding time period was determined by integrating the curve of heat flow from the beginning to the determined time [35–37], so the degree of cure was calculated in the form [38]:

$$\alpha = \frac{\Delta H_t}{\Delta H_{total}} \quad (1)$$

where  $\alpha$  is the degree of cure,  $\Delta H_t$  is the reaction heat at time  $t$ , and  $\Delta H_{total}$  is the total reaction heat of reaction.

#### 2.2.3. Glass transition temperature

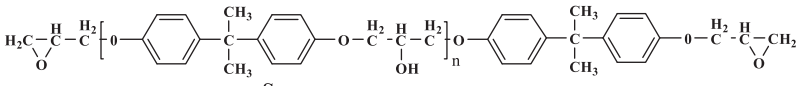
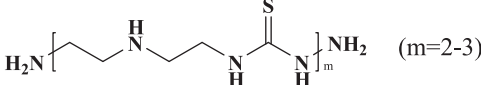
The reactants E-44 and TU-DETA were mixed under –18 °C with the mass ratio of 6:1 from –50 °C to 250 °C firstly and then re-scanning the completely cured sample at 10 °C min<sup>-1</sup>, the glass transition temperature ( $T_g$ ) was found to be at a temperature of  $116 \pm 2$  °C, presented in Fig. 1.  $T_g$  was determined as the midpoint of the step (defined according to ASTM E 2602) [16] in the curve presenting curing exotherm during the dynamic re-scanning.

## 3. Results and discussion

### 3.1. Determining the dosage of curing agent

For the sake of determining the optimum dosage of curing agent, a series of different mass ratios of E-44 and TU-DETA uncured component samples for DSC measurement was weighed, wherein the upward direction of the peaks in the curve representing exothermic reaction. The change in heat flow versus temperature and time during cure at the heating rate of 10 °C min<sup>-1</sup> is shown in Fig. 2. A straight baseline was used to integrate the peak of heat flow versus time to give the reaction heat. The value of heat released is listed in Table 2.

**Table 1**  
Structures of the chemicals.

Materials	Molecular structures
E-44	
TU-DETA	 (m=2-3)

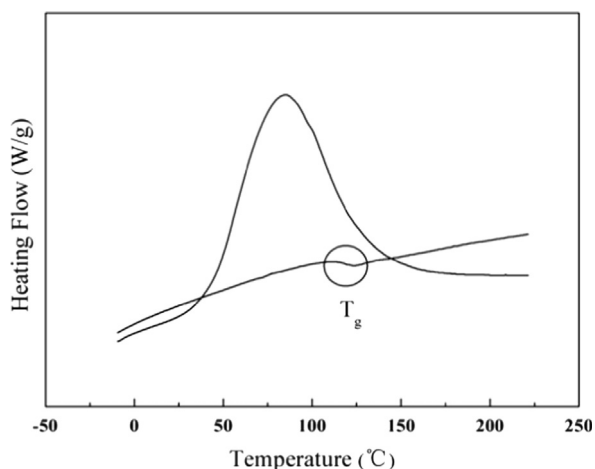


Fig. 1. Heat flow versus temperature in DSC scans of uncured and completely cured samples.

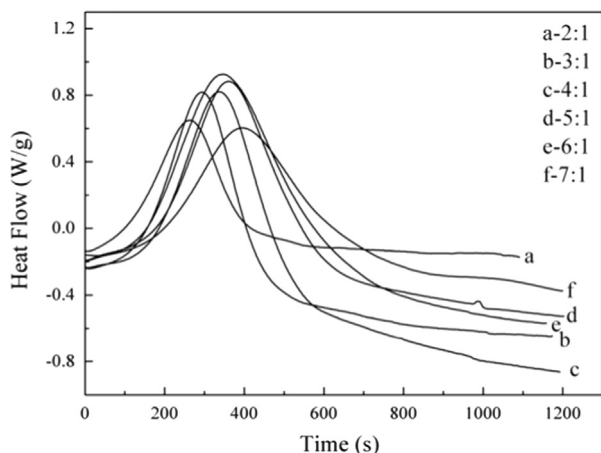


Fig. 2. DSC curves of curing systems with different mass ratios of matrix resin and curing agent.

Table 2  
Reaction heat of different curing systems.

E-44:TU-DETA	2:1	3:1	4:1	5:1	6:1	7:1
$\Delta H$ (J/g)	179.614	319.463	391.420	447.592	465.684	306.830

From Table 2, we knew that with the mass ratio of E-44 and TU-DETA increasing, the heat release increased firstly and then decreased, therefore, we could make a conclusion that the optimum mass ratio of E-44 and TU-DETA was 6:1 when the value of heat release was the largest.

### 3.2. Kinetic analysis of dynamic scanning

The change in heat flow versus temperature and time during curing at different heating rates is presented in Fig. 3(a) and (b). The shapes of the exotherm were heating rate-dependent. The peak temperature,  $T_p$ , the onset of cure temperature,  $T_{onset}$ , the endset of cure temperature,  $T_{endset}$  (defined according to ASTM E2041) [16], were determined by Fig. 3(a), choosing the example with the rate of  $10^\circ\text{C min}^{-1}$  (Fig. 4) to demonstrate how to determine the three temperatures. In this study, a straight baseline was used to integrate heat flow versus time to give the reaction

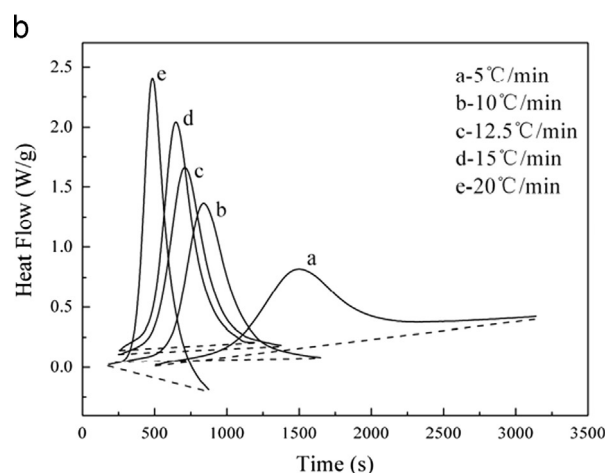
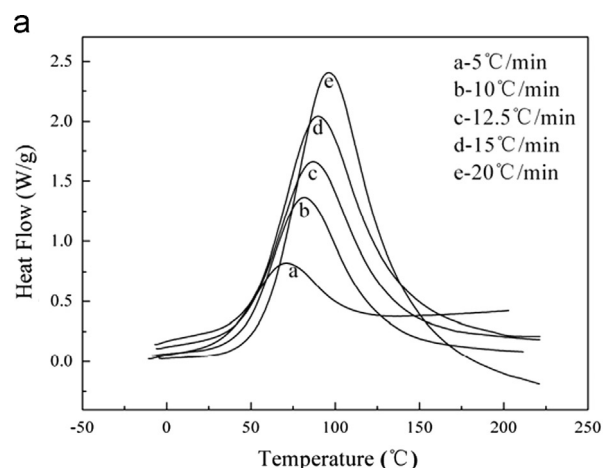


Fig. 3. Heat flow at different heating rates during dynamic scanning versus (a) temperature and (b) time (between onset and end of cure).

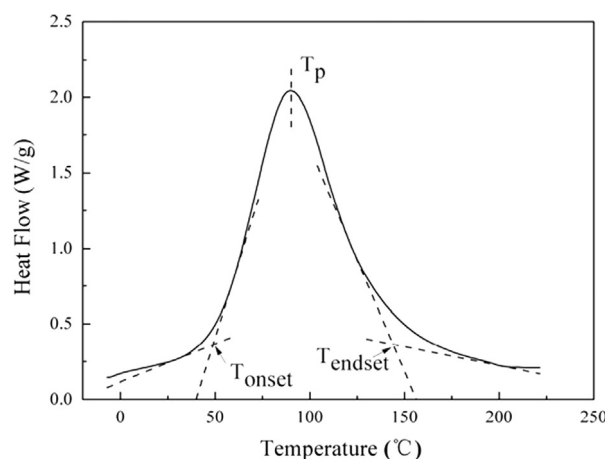


Fig. 4. Determining  $T_{onset}$ ,  $T_p$ ,  $T_{endset}$  of heat flow versus temperature in DSC scans of uncured sample with a heating rate of  $10^\circ\text{C min}^{-1}$ .

heat, as presented in Fig. 3(b). The total reaction heat,  $\Delta H_T$ , was also heating rate-dependent. The curing degree,  $\alpha$ , was calculated by Eq. (1). By differentiating the curing degree versus time or temperature, the relationship between the cure rate and time or temperature was determined. These data was used as the source data to simulate the dynamic curing process. The results are listed in Table 3.

**Table 3**  
Dynamic scanning results at different heating rates.

Parameter	$dT/dt$ ( $^{\circ}\text{C min}^{-1}$ )				
	5	10	12.5	15	20
$\Delta H_T$ (J/g)	464.008	465.684	467.393	486.660	470.426
$T_{onset}$ ( $^{\circ}\text{C}$ )	33.92	42.17	46.53	50.61	57.07
$T_p$ ( $^{\circ}\text{C}$ )	71.16	81.68	86.81	89.86	96.22
$T_{endset}$ ( $^{\circ}\text{C}$ )	108.44	127.83	133.78	140.32	153.81
$\alpha_p$ (%)	0.398	0.404	0.419	0.413	0.409
$(d\alpha/dt)_p$ ( $\text{min}^{-1}$ )	0.084	0.168	0.195	0.231	0.316
$(d\alpha/dT)_p$ ( $\text{K}^{-1}$ )	0.0175	0.0170	0.0159	0.0157	0.0162

### 3.3. Theoretical approaches

#### 3.3.1. Dynamic modeling

All kinetic studies can start with the basic equation. In general terms, the cure kinetics can be described by a rate law given by the following expression [39]:

$$\frac{d\alpha}{dt} = k(T)f(\alpha) \quad (2)$$

where  $\alpha$  is the curing degree,  $d\alpha/dt$  is curing rate,  $k$  is the Arrhenius rate constant, and  $f(\alpha)$  is a function that depends on the reaction mechanism. Furthermore, the rate constant  $k(T)$  can be expressed by the Arrhenius equation [40]:

$$k(T) = Ae^{-(E_a/RT)} \quad (3)$$

where  $A$  is the pre-exponential factor,  $E_a$  is the apparent activation energy (J/mol),  $R$  is the gas constant,  $R=8.314$  J/(mol k), and  $T$  is the absolute temperature. Substituting Eq. (3) into Eq. (2)

$$\frac{d\alpha}{dt} = Ae^{-(E_a/RT)}f(\alpha) \quad (4)$$

For a dynamic curing process with constant heating rate, the temperature increased linearly with the increment of cure time  $t$ . The relationship between  $d\alpha/dt$  and  $d\alpha/dT$  can be expressed as

$$\frac{d\alpha}{dt} = \left(\frac{dT}{dt}\right) \frac{d\alpha}{dT} = \beta \frac{d\alpha}{dT} \quad (5)$$

where  $\beta = dT/dt$  is the constant heating rate.

Substituting Eq. (5) into Eq. (4) and rearranging:

$$\beta = A \left(\frac{d\alpha}{dT}\right)^{-1} f(\alpha) e^{-(E_a/RT)} \quad (6)$$

Basically, curing of epoxy resins may exhibit two different behaviors,  $n$ th order or autocatalytic. Two distinguished methods existed. Firstly: observing the plot. The main difference is that  $n$ th order modeling exhibits the maximum of curing rate at the beginning of the reaction, while autocatalytic modeling show a delayed peak, which occurs during the curing process [41]. Secondly: a statistic methodology [42]. Defining a special function  $y(\alpha)$  which can be expressed as follows [43,44]:

$$y(\alpha) = \left(\frac{d\alpha}{dT}\right) e^{E_a/RT} \quad (7)$$

$d\alpha/dt$  can easily be obtained by simple transformation of experiment data,  $E_a$  can be obtained by linear fitting (elucidated in the following section). The shape of the function  $y(\alpha)$  (presented in Fig. 5) was plotted by normalizing it within the [0,1] interval. Based on the responses shown in Figs. 3 and 5, which exhibited a delayed peak, an autocatalytic behavior was assumed, for the autocatalytic model with the initial cure rate of zero, the term  $f(\alpha)$  may have the form [45–47]

$$f(\alpha) = \alpha^m(1-\alpha)^n \quad (8)$$

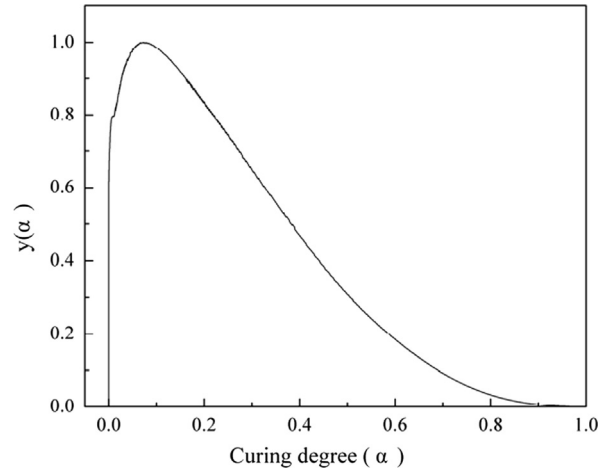


Fig. 5. Shape of the function of  $y(\alpha)$  versus curing degree  $\alpha$ .

where  $m$  and  $n$  are the reaction orders, and  $m+n$  are the overall reaction order. Substituting Eq. (8) into Eq. (6)

$$\beta = A \left(\frac{d\alpha}{dT}\right)^{-1} \alpha^m(1-\alpha)^n e^{-(E_a/RT)} \quad (9)$$

Taking the natural logarithm on both sides of Eq. (9)

$$\ln\left(\frac{dT}{dt}\right) = \ln A - \ln\left(\frac{d\alpha}{dT}\right) + \ln[\alpha^m(1-\alpha)^n] + \left(\frac{-E_a}{R}\right) \frac{1}{T} \quad (10)$$

At peak temperature,  $T_p$ , the derivative of curing rate versus temperature equals zero, which means that the derivative of curing degree versus temperature is a constant value regardless of heating rate.  $((d\alpha/dt)/dT)_{T=T_p} = 0$ , means  $(d\alpha/dt)_{T=T_p} = c$ ,  $dt/dT \cdot d\alpha/dt = dt/dT \cdot c \Leftrightarrow d\alpha/dT = c'$ , where  $c$  and  $c'$  are constants. The term  $\ln[\alpha^m(1-\alpha)^n]$  at the peak temperature changed with the heating rate, but its value was very small compared to term  $\ln A$  [14]. Based on the above considerations, the general linear form of Eq. (10) can be written as

$$\ln(\beta) = K + \left(\frac{-E_a}{R}\right) \frac{1}{T_p} \quad (11)$$

where  $K$  is the intercept of Eq. (10),  $[-(E_a/R)]$  is the slope of the plot  $\ln(\beta)$  versus  $1000/T_p$  (presented in Fig. 6).

$$K = \ln \bar{A} - \ln\left(\frac{d\alpha}{dT}\right)_p + \ln[\alpha_p^m(1-\alpha_p)^n] \quad (12)$$

where  $\bar{A}$  is the average value of the pre-exponential factors at the five heating rates. The terms  $T_p$ ,  $(d\alpha/dT)_p$  and  $\alpha_p$  are the absolute temperature, derivative of curing degree to temperature, and curing degree at the exothermic peak, respectively. Their values are shown in Table 3.

Eq. (12) can be rearranged to obtain an expression for the average pre-exponential factor  $\bar{A}$

$$\bar{A} = \frac{e^K (d\alpha/dT)_p}{\alpha_p^m(1-\alpha_p)^n} \quad (13)$$

Having obtained the average pre-exponential factor  $\bar{A}$ , based on this value and Sun et al. [15], heating rate-specific values  $A_f$  were obtained as follows:

$$A_f = C_f \bar{A} = C_f \frac{e^K (d\alpha/dT)_p}{\alpha_p^m(1-\alpha_p)^n} \quad (14)$$

where  $C_f$  is the heating rate-dependent correction factor of  $\bar{A}$ ,  $(d\alpha/dT)_p$  and  $\alpha_p$  are derivatives of curing degree to temperature and the curing rate at the exothermic peak, respectively, as given in Table 3. Substituting Eqs. (14) and (8) into the basic curing rate

Eq. (4), the curing rate for an autocatalytic model yields to

$$\frac{d\alpha}{dt} = C_f e^{K_p} \left( \frac{d\alpha}{dT} \right)_p e^{-(E_a/RT)} \frac{\alpha^m (1-\alpha)^n}{\alpha_p^m (1-\alpha_p)^n} \quad (15)$$

The correction factor  $C_f$  as well as the reaction orders,  $m$  and  $n$ , were determined from Eq. (15) using the multiple nonlinear least square regression method based on the Levenberg–Marquardt algorithm, the results are listed in Table 4.

### 3.3.2. Isoconversional methods

All isoconversional methods are based on the isoconversional principle, stating that the reaction rate at constant extent of conversion is only a function of temperature [6,29,48]. It can be elucidated by taking the logarithmic derivative of the reaction rate (Eq. (2)) at  $\alpha = \text{const}$

$$\left[ \frac{\partial \ln(d\alpha/dt)}{\partial T^{-1}} \right]_{\alpha} = \left[ \frac{\partial \ln k(T)}{\partial T^{-1}} \right]_{\alpha} + \left[ \frac{\partial \ln f(\alpha)}{\partial T^{-1}} \right]_{\alpha} \quad (16)$$

where the subscript  $\alpha$  is the values related to a given extent of curing degree. Based on the basic assumption of isoconversional methods  $f(\alpha)$  is constant,  $\alpha = \text{const}$ , the second term in the right hand side of Eq. (16) is zero, thus

$$\left[ \frac{\partial \ln(d\alpha/dt)}{\partial T^{-1}} \right]_{\alpha} = -\frac{E_a}{R} \quad (17)$$

Thus, a model-free value of the apparent energy  $E_a$  can be obtained for each  $\alpha$  value.

### 3.3.3. Advanced isoconversional method

An advanced isoconversional method (NLN Vyazovkin method) developed by Vyazovkin [30–32] is taken into account for the variation of  $E_a$  in the computation of the temperature integral. The  $E_a$  value can be determined at any particular value of  $\alpha$  by

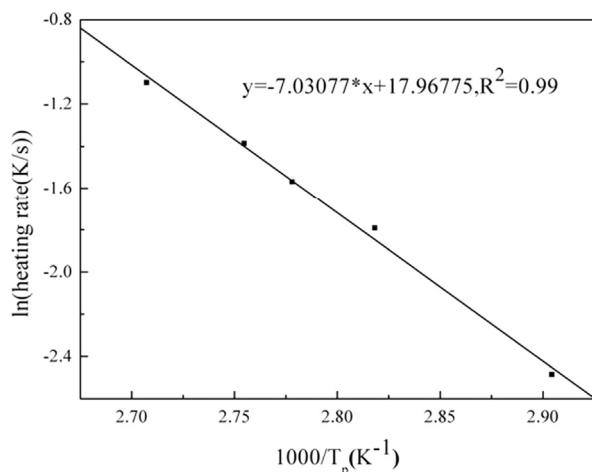


Fig. 6. Plots of logarithm heating rate versus reciprocal of absolute exothermal peak temperature.

Table 4

Kinetic parameters obtained from the autocatalytic dynamic model.

Model	Parameter	$dT/dt$ ( $^{\circ}\text{C min}^{-1}$ )					$R^2$
		5	10	12.5	15	20	
Unmodified	$E_a$ ( $\text{KJ mol}^{-1}$ )	58.454					0.99
	$A$ ( $\text{min}^{-1}$ )	235209680.4					0.99
Modified	$m$	0.25	0.20	0.14	0.13	0.19	0.99
	$n$	2.49	2.14	2.12	2.09	2.12	0.99
	$C_f$	0.99737	1.08955	1.06009	1.04571	0.93925	0.99
	$A_f$ ( $\text{min}^{-1}$ )	295754682	256353201.3	229337883.2	214045565.9	209643350.6	0.99

minimizing the following function [6,29,30,49]:

$$\Phi(E_a) = \sum_{i=1}^n \sum_{j \neq i}^n \frac{I(E_a, T_{\alpha,i}) \beta_j}{I(E_a, T_{\alpha,j}) \beta_i} \quad (18)$$

where  $I$  is evaluated over small intervals to take into account for the variation of  $E_a$  [29]

$$I(E_a, T_i(t_{\alpha})) \equiv \int_{t_{\alpha-\Delta\alpha}}^{t_{\alpha}} e^{-(E_a/RT_i(t))} dt \quad (19)$$

For a linear heating program, Eq. (19) can be expressed with the Doyle's approximation [50].

$$I(E_a, T) \approx \frac{E_a}{R} e^{-5.331 - 1.052 E_a/RT} \quad (20)$$

For a given value of  $\alpha$  and a set of experiments performed under different heating rates  $\beta_i$  ( $i=1, \dots, 5$ ).

$$(A_{\alpha}/\beta_1) I(E_a, T_{\alpha,1}) = \dots = (A_{\alpha}/\beta_5) I(E_a, T_{\alpha,5}) \quad (21)$$

After removing  $A_{\alpha}$ , Eq. (21) can be expressed as a minimum value

$$\sum_{i=1}^n \sum_{j \neq i}^n [I(E_a, T_{\alpha,i}) \beta_j] / [I(E_a, T_{\alpha,j}) \beta_i] = \min \quad (22)$$

where  $i$  is an ordinal number representing experiments performed at different heating rates,  $\beta_i$ ,  $T_{\alpha,i}$  is the temperature at a given value of  $\alpha$  in an experiment performed at  $\beta_i$ . We substituted experimental values of  $T_{\alpha}$  and  $\beta$  into Eq. (22) and varying  $E_a$  to reach the minimum  $E_a$  value at a given value of  $\alpha$  [30]. Mathematica software was used to compute  $E_a$  value for each value of  $\alpha$  lying between 0.05 and 0.95 with a step of 0.01.

### 3.3.4. Compensation parameters

The activation energy and pre-exponential factors may change with each extent of  $\alpha$ , temperature or the reaction model used [29]. The method of invariant kinetic parameters that are apparent activation parameters [51–55] is “compensation effect”. The correlation of invariant apparent activation energy and pre-exponential factor can be expressed by the following equation:

$$\ln(A_i) = \frac{E_{ai}}{RT} + \ln \left[ \frac{(d\alpha/dt)}{f(\alpha)} \right]_i = a + b E_{ai} \quad (23)$$

where  $a$  and  $b$  are compensation parameters and the subscript  $i$  is an ordinal number representing experiments performed at different heating rates. For differential DSC data, the ABS method was natural to use. In order to compute the compensation parameters, special values of the exponents  $m$  and  $n$  of the well-known simplified Sestak–Berggren equation were used (see ref. [29], models 15–18 of Table 1). These are as follows:  $m=1, n=2$ ;  $m=2, n=1$ ;  $m=1, n=1$ ;  $m=0.5, n=1.5$ ;  $m=0$ , and  $n=2$  (model 14).  $\ln A_i$  and  $E_{ai}$  were evaluated for models using the ABS method for  $0.20 < \alpha < 0.80$ . The results for five heating rates (5, 10, 12.5, 15,  $20^{\circ}\text{C min}^{-1}$ ) are listed in Table 5. Then the values of compensation parameters can be obtained by linear fitting  $\ln A_i$  and  $E_{ai}$ . The results are listed in Table 6.

**Table 5**  
Kinetic parameters obtained with the differential ABS method.

Reaction Models	$\beta = 5\text{ }^{\circ}\text{C min}^{-1}$			$\beta = 10\text{ }^{\circ}\text{C min}^{-1}$			$\beta = 12.5\text{ }^{\circ}\text{C min}^{-1}$			$\beta = 15\text{ }^{\circ}\text{C min}^{-1}$			$\beta = 20\text{ }^{\circ}\text{C min}^{-1}$		
	$E_a$ (KJ mol <sup>-1</sup> )	$\ln(A)$ (s <sup>-1</sup> )	$R^2$	$E_a$ (KJ mol <sup>-1</sup> )	$\ln(A)$ (s <sup>-1</sup> )	$R^2$	$E_a$ (KJ mol <sup>-1</sup> )	$\ln(A)$ (s <sup>-1</sup> )	$R^2$	$E_a$ (KJ mol <sup>-1</sup> )	$\ln(A)$ (s <sup>-1</sup> )	$R^2$	$E_a$ (KJ mol <sup>-1</sup> )	$\ln(A)$ (s <sup>-1</sup> )	$R^2$
$\alpha(1-\alpha)^2$	18.0738	1.7210	0.9850	24.0126	4.2516	0.9686	24.5502	4.4789	0.9750	24.0005	4.3840	0.9757	22.8120	4.1474	0.9693
$\alpha^2(1-\alpha)$	-47.241	-20.7444	0.9887	-47.516	-19.6386	0.9841	-44.6118	-18.3245	0.9871	-44.9874	-18.1476	0.9878	-50.1943	-19.2260	0.9842
$\alpha(1-\alpha)$	-15.774	-10.6914	0.9866	-12.6503	-8.7639	0.9940	-10.8788	-7.9728	0.9840	-11.3564	-7.9343	0.9800	-14.8874	-8.6931	0.9893
$\alpha^{0.5}(1-\alpha)^{1.5}$	16.884	0.54126	0.9642	23.114	3.1812	0.9944	23.7021	3.4289	0.9937	23.1374	3.33147	0.9920	21.6157	2.9937	0.9890
$(1-\alpha)^2$	49.541	15.8683	0.9912	58.8783	15.12623	0.9981	58.2831	14.8306	0.9983	57.6314	14.59725	0.9979	58.1189	14.6804	0.9968

The apparent activation energy and pre-exponential factors for each value of  $\alpha$  lying between 0.05 and 0.95 with a step of 0.01 are presented in Fig. 7.

As shown in Fig. 7, the apparent activation energy  $E_a$  increased gradually with the increment of curing degree, owing to the further energy required to increase the mobility of both reactants and products during the late stages of the curing process [15,16].

3.3.5. Fitting results

Once the kinetic parameters  $A$ ,  $E_a$ ,  $m$  and  $n$  where we use average pre-exponential factor and average activation energy for the whole reaction process had been estimated, the curing degree was calculated as a function of the temperature by solving Eq. (15)

$$\frac{d\alpha}{dT} = \frac{A_f}{dT/dt} e^{-(E_a/RT)} \alpha^m (1-\alpha)^n \tag{24}$$

By integrating the term  $d\alpha/dT$  as a function of the absolute temperature  $T$ , the curing degree  $\alpha$  versus temperature could be obtained. The result for the heating rate of 20 °C min<sup>-1</sup> with and without modification of the pre-exponential factor is presented in Fig. 8. The modeling curves compare well with the experimental results, especially with modification of the pre-exponential factor.

Fig. 9 shows the curing rate versus temperature for the heating rates of 5, 10, 12.5, 15, 20 °C min<sup>-1</sup>. Similarly, the autocatalytic model

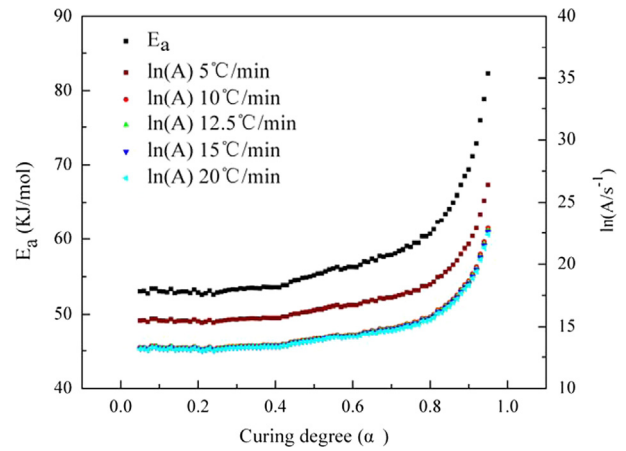


**Fig. 7.** Left Y-axis, solid squares:  $E_a$ -dependency from the NLN Vyazovkin method. Right Y-axis:  $\ln A$ -dependencies obtained with ABS compensation parameters of the heating rates of 5, 10, 12.5, 15, 20 °C min<sup>-1</sup>.

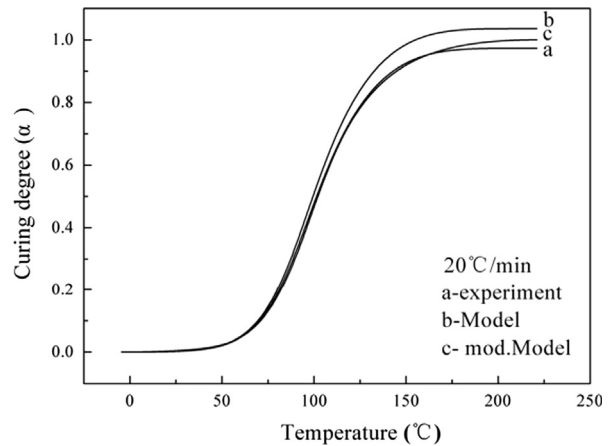


**Fig. 8.** Curing degree versus temperature: experimental result and the autocatalytic model result with and without modified pre-exponential factor of 20 °C min<sup>-1</sup>.

**Table 6**  
Compensation parameters obtained with the ABS method.

Method	$\beta=5\text{ }^{\circ}\text{C min}^{-1}$			$\beta=10\text{ }^{\circ}\text{C min}^{-1}$			$\beta=12.5\text{ }^{\circ}\text{C min}^{-1}$			$\beta=15\text{ }^{\circ}\text{C min}^{-1}$			$\beta=20\text{ }^{\circ}\text{C min}^{-1}$		
	$b$ (mol KJ <sup>-1</sup> )	$a$	$R^2$	$b$ (mol KJ <sup>-1</sup> )	$a$	$R^2$	$b$ (mol KJ <sup>-1</sup> )	$a$	$R^2$	$b$ (mol KJ <sup>-1</sup> )	$a$	$R^2$	$b$ (mol KJ <sup>-1</sup> )	$a$	$R^2$
ABS	0.37259	-4.26196	0.9876	0.32909	-4.18572	0.999	0.32464	-4.02597	0.9989	0.32152	-3.86777	0.9988	0.31538	-3.58285	0.999

**Table 7**  
Isothermal scanning results at different temperatures.

Parameter	$T_{cure}$ (°C)							
	10	15	25	35	45	60	80	
$\Delta H_{iso}$ (J/g)	296.515	335.346	434.043	441.546	468.886	470.834	470.834	
$\alpha$ (%)	0.630	0.712	0.922	0.938	0.996	1	1	
$t_{1/2}$ (h)	2.40	1.74	0.99	0.54	0.33	0.15	0.06	

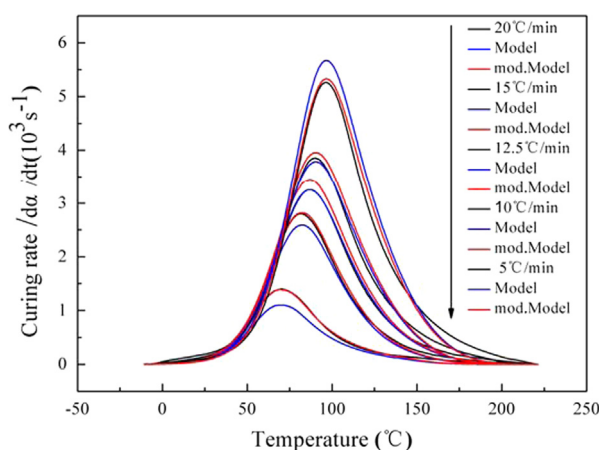


**Fig. 9.** Curing rate versus temperature: experimental results and the autocatalytic model results with and without modified pre-exponential factor for five heating rates.

with modification of the pre-exponential factor provides better and more accurate results than the model without modification.

### 3.4. Kinetic analysis of isothermal scanning

#### 3.4.1. Characters of curing process

During the curing process, the instrument recorded the heat flow change with the cure time. A series of isothermal measurements were performed starting from 10 °C to 80 °C. To achieve almost constant heat flow in the late cure stage, the measurement time was set long enough. The heat flow versus time of isothermal scans at all temperatures is presented in Fig. 10(a) and (b). Again, the value of heat released during isothermal scanning,  $\Delta H_{iso}$ , was determined by the area under each isothermal curve considering the plateau as horizontal baseline. The results are presented in Table 7.

In this experiment, the sample used was fresh and uncured. The curing degree,  $\alpha$  (see Table 7), could be calculated as  $\Delta H_{iso} / \Delta H_T$ , where  $\Delta H_T = 470.834$  J/g was the average heat reactions of the dynamic scanning under five heating rate. The curing rate at each sampling time and temperature was calculated by differentiating the curing degree to time.

Half-life,  $t_{1/2}$  (see Table 7), is the time required to reach 50% curing degree at a certain cure temperature. The 60-min half-life temperature was found to be 25 °C.

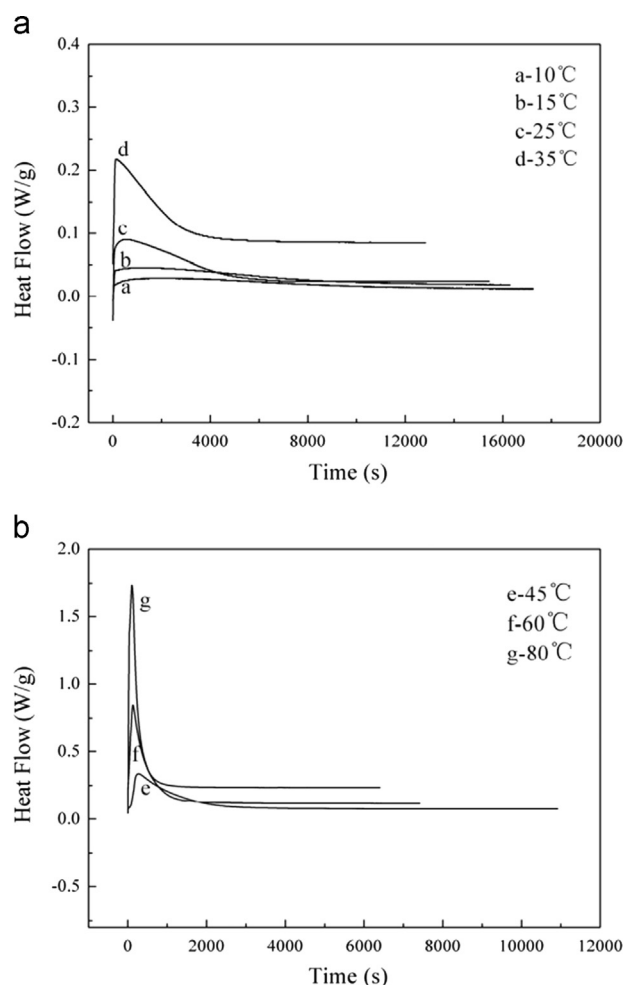


**Fig. 10.** Heat flow versus time at different isothermal curing temperatures: (a) 10 °C, 5 °C, 25 °C, 35 °C; (b) 45 °C, 60 °C, 80 °C.

#### 3.4.2. Isothermal modeling

Kamal et al. [56,57] have showed that a more general model taking non-zero values of the initial curing rate into account represents adequately the cure kinetics of epoxy for the isothermal modeling

$$\frac{d\alpha}{dt} = (k_1 + k_2\alpha^m)(1 - \alpha)^n \quad (25)$$

**Table 8**  
Kinetic parameters obtained from the autocatalytic isothermal model.

T (°C)	k (s <sup>-1</sup> )	m	n	m+n	R <sup>2</sup>	E <sub>a</sub> (KJ/mol)	A (s <sup>-1</sup> )	R <sup>2</sup>
10	0.000131	0.169	1.616	1.785	0.99	56.863	3548799.73	0.99
15	0.000164	0.151	1.480	1.631	0.99			
25	0.000444	0.173	1.045	1.218	0.99			
35	0.000608	0.185	1.695	1.880	0.99			
45	0.00155	0.361	2.002	2.363	0.99			
60	0.00462	0.421	2.596	3.017	0.99			
80	0.0154	0.558	2.942	3.500	0.99			

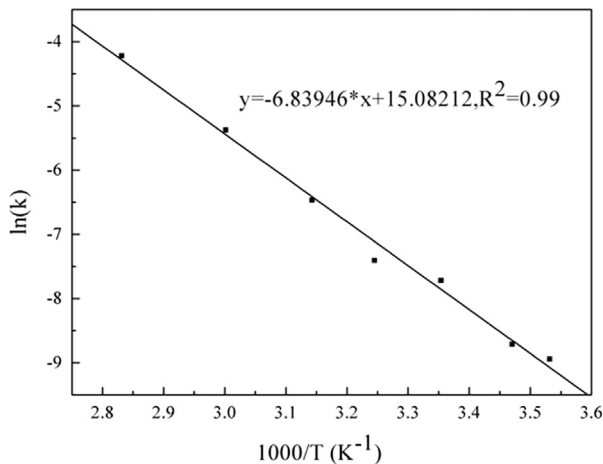


**Fig. 11.** Logarithms of the rate constants versus temperature.

Where  $k_1$  and  $k_2$  are curing rate constants,  $m$  and  $n$  are reaction orders independent of temperature. This equation has been widely used in the literature to represent the curing of thermosetting resin [58,59].

In this experiment, we did not take the nonisothermal heat-up period which was very short into consideration, that is to say, at the beginning of the reaction at  $t=0$ , the term curing rate,  $d\alpha/dt$ , is zero for all temperatures, thus  $k_1=0$ . Eq. (25) can be simplified to Eq. (26) [18,60,61].

$$\frac{d\alpha}{dt} = k\alpha^m(1-\alpha)^n \quad (26)$$

The reaction parameters  $k$ ,  $m$  and  $n$  can be obtained by fitting the isothermal data with nonlinear least square regression method based on the Levenberg–Marquardt algorithm using Mathematica software.

The kinetic rate constant  $k$  follows an Arrhenius temperature dependence. By plotting the logarithms of the rate constant,  $\ln k$ , versus  $1000/T$ , the activation energy  $E_a$ , and logarithms of the pre-exponential factor,  $\ln A$ , were obtained from the slope and the intercepts, respectively, presented in Fig. 11. The values for the rate constants and reaction orders at different temperatures are listed in Table 8. The cure reaction orders  $m$  and  $n$  increased with the increment of temperature overall. Similarly, the rate constant  $k$  increased with the increment of temperature (the rate constant  $k$  has the same tendency of reaction orders  $m$  and  $n$ ), which can be expressed by the following Arrhenius equation:  $k = Ae^{-E_a/RT}$ . Comparing the diffusion factor to that of previously reported epoxy resins cured at higher temperature, we found that the diffusion factor is similar. It is owing to the fact that diffusion-controlled only modified the later curing stages and the modification effect was the same.

In the late stage of the curing process, as the resin has cross-linked, the movement of the reacting groups was hindered, thus

**Table 9**  
Diffusion control parameters obtained from the autocatalytic isothermal model.

T (°C)	C	$\alpha_c$	R <sup>2</sup>
10	29.440	0.592	0.99
15	28.673	0.675	0.99
25	125.331	0.912	0.99

the rate of cure was controlled by diffusion rather than by chemical factors. To consider diffusion effect, a diffusion factor  $g(\alpha)$  was applied by Khanna and Chanda [18,61] and defined as the ratio  $k_e/k_c$ , where  $k_c$  is the rate constant for chemical kinetics,  $k_e$  is the overall effective rate constant and  $k_d$  is the diffusion controlled rate constant.  $k_e$  can be expressed in terms of  $k_d$  and  $k_c$  by the relation

$$\frac{1}{k_e} = \frac{1}{k_d} + \frac{1}{k_c} \quad (27)$$

where  $k_d$  can be expressed in terms of  $k_c$  by the relation

$$k_d = k_c \exp[-c(\alpha - \alpha_c)] \quad (28)$$

where  $\alpha_c$  is the critical curing degree at which diffusion control initiates and  $C$  is an empirical constant. By combining Eq. (27) with Eq. (28), we can obtain the diffusion factor  $g(\alpha)$ :

$$g(\alpha) = \frac{k_e}{k_c} = \frac{1}{1 + \exp[c(\alpha - \alpha_c)]} \quad (29)$$

When  $\alpha$  is much smaller than the critical value,  $\alpha \ll \alpha_c$ , then  $g(\alpha)$  approximates unity, the reaction is kinetically controlled and the effect of diffusion is negligible. As  $\alpha$  approaches  $\alpha_c$ ,  $g(\alpha)$  begins to decrease and approaches zero as the reaction effectively stops. The effective reaction rate at any curing degree is equal to the chemical reaction rate multiplying by  $g(\alpha)$ .

To obtain these two parameters  $C$  and  $\alpha_c$ , the experimental results were non-linearly re-fitted based on the Levenberg–Marquardt algorithm using Mathematica software with known kinetic parameters. The results were listed in Table 9.

As shown in Table 9, the empirical constant  $C$  and the critical curing degree  $\alpha_c$  increased when the curing temperature was increased. At high temperatures ( $> 35^\circ\text{C}$ ), we did not found the diffusion control.

The relationship between the curing rate and the curing degree was presented in Fig. 12 at temperatures between 10 and 80 °C. Good agreement between experimental data and the autocatalytic model with diffusion control was found over the curing temperature ranging from 10 °C to 25 °C. Similarly, experimental results were accurately simulated by the autocatalytic model without diffusion control.

### 3.4.3. Analysis of nonlinear regression

Curing kinetics of nonlinear regression has the form  $y = f(x; k, m, n) + \varepsilon$ , assuming the modeling complies with Gauss–Markov theorem,  $y$  obeys Normal distribution  $N(f(x; k, m, n), \sigma^2 I)$ ,



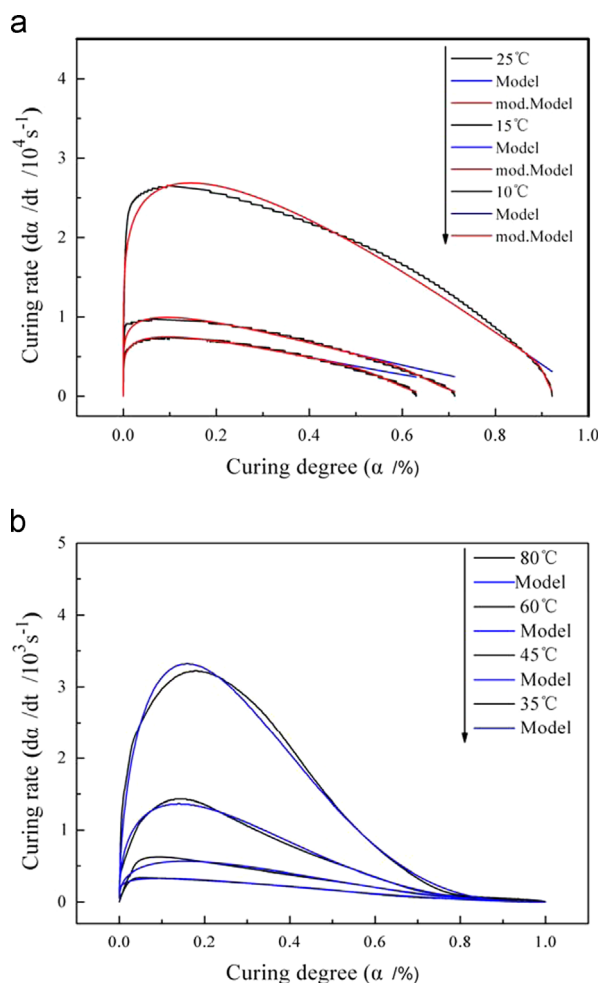


**Fig. 12.** Curing rate versus curing degree: experimental results and the autocatalytic model results with or without diffusion for different isothermal temperatures: (a): 10–25 °C; (b): 35–80 °C.

error  $\varepsilon$  satisfies i.i.d.  $N$  (independent of the Normal distribution) and  $N(0, \sigma^2)$ . In the initial value of parameters, using a first-order of Taylor formula, the expansion of the model function is approximately linear form and applies the least squares Levenberg–Marquardt algorithm to this linear function approximation, moreover, using the experimental data of each temperature to carry on fitting. Since the sample size of the experimental data is so large, therefore, large sample under the linear approximation of nonlinear models show enough significance, estimator of model parameters is unbiased with minimum variance.

According to the M.J. Box deviation algorithm, the results of the size of the fitting parameters are as follows in Table 10.

As shown in Table 10, the values of the deviation size and the percentage of parameter estimation are less than 1%. According to empirical rule of the percentage deviation of 1%, when the percentage of deviation does not reach the upper limitation of 1%, it can be concluded that the least squares fitting of nonlinear which carries on linear approximation by Taylor formula has a satisfactory effect.

#### 4. Conclusions

Kinetic researches on low-temperature cure of epoxy adhesive was experimentally and analytically investigated by means of differential scanning calorimetry analysis on both isothermal and dynamic scanning. The following conclusions were drawn:

**Table 10**  
Results of the size of the fitting parameters.

Temperature (°C)	Estimated variance	Parameter bias		
		$k$	$m$	$n$
10	3.59E–11	5.71E–9	0.00000397	0.0000134
15	4.88E–11	4.76E–9	0.00000369	0.0000108
25	1.39E–10	4.58E–9	0.00000268	0.00000501
35	8.40E–11	4.27E–9	0.00000162	0.00000414
45	4.54E–10	3.76E–8	0.00000513	0.0000130
60	9.99E–10	1.41E–7	0.00000549	0.0000163
80	2.39E–9	5.72E–7	0.00000723	0.0000191

- (1) For dynamic curing section, an advanced isoconversional method was taken into account for computing the minimum apparent activation energy  $E_a$  value for each value of  $\alpha$  lying between 0.05 and 0.95 with a step of 0.01. The correlation of invariant apparent activation energy and pre-exponential factor were expressed by “compensation parameters” equation.
- (2) Curing did take place at low temperatures of 10–15 °C but it was difficult to reach complete reaction over a reasonable experiment time period because the curing process significantly decelerated owing to the effects of material vitrification and the associated diffusion controlled in the late isothermal curing stages in isothermal experimental. The cure reaction orders  $m$  and  $n$  increased with the increment of temperature overall. Similarly, the rate constant  $k$  increased with the increment of temperature. Comparing the diffusion factor to that of previously reported epoxy resins cured at higher temperature, we found that the diffusion factor is similar. It is owing to the fact that diffusion-controlled only modified the later curing stages and the modification effect was the same.
- (3) Existing dynamic and isothermal curing phenomenological autocatalytic models developed for hot-curing adhesives proved applicable to simulate the curing behavior of the cold-curing adhesive even at low temperatures. However, a heating rate-dependent pre-exponential factor and diffusion control had to be taken into account. The modified modeling with diffusion controlled was much more accurate simulate to the experimental data by low-temperature isothermal curing adhesive, similarly, the modified modeling with heating rate-specific pre-exponential factor agreed well with experimental data.
- (4) Analysis of nonlinear regression was carried on the isothermal modeling, results showed that the nonlinear least squares fitting which carried out on linear approximation by Taylor formula had a satisfactory effect.

#### Acknowledgments

The authors are grateful for the financial support of the Project funded by Ministry of Education Key Laboratory for the Synthesis and Application of Organic Functional Molecules.

#### References

- [1] Pham HQ, Marks MJ. Epoxy resins. In: Mark HF, editor. Encyclopedia of polymer science and technology. New York: John Wiley & Son; 2004. p. 678–804.
- [2] Petrie EM. Epoxy adhesives formulations. New York: McGraw-Hill; 2006.
- [3] Li Q, Li XY, Meng Y. Curing of DGEBA epoxy using a phenol-terminated hyperbranched curing agent: cure kinetics, gelation, and the TTT cure diagram. Thermochim Acta 2012;549:69–80.
- [4] López J, López-Bueno I, Nogueira P, Ramírez C, Abad MJ, Barral L, et al. Effect of poly(styrene-co-acrylonitrile) on the curing of an epoxy/amine resin. Polymer 2001;42:1669–77.

- [5] Ueki T, Nishijima S, Izumi Y. Designing of epoxy resin systems for cryogenic use. *Cryogenics* 2005;45:141–8.
- [6] Vyazovkina S, Burnhamb AK, Criado JM, Pérez-Maquedac LA, Popescud C, Sbirrazzuoli N. ICTAC Kinetics Committee recommendations for performing kinetic computations on thermal analysis data. *Thermochim Acta* 2011;520:1–19.
- [7] Atkins P, de Paula J. *Physical chemistry*. 9th ed. New York: W.H. Freeman; 2010.
- [8] Brown ME. *Introduction to thermal analysis*. 2nd ed. Dordrecht: Kluwer; 2001.
- [9] Skordos AA, Partidge IK. Cure kinetic modeling of epoxy resins using a non-parametric numerical procedure. *Polym Eng Sci* 2001;41:793–805.
- [10] Gutowski TGP. *Advanced composites manufacturing*. New York: Wiley-Interscience; 1997.
- [11] Ramis X, Cadenato A, Morancho JM, Salla JM. Curing of a thermosetting power coating by means of DMTA, TMA and DSC. *Polymer* 2003;44:2067–79.
- [12] Karkanas PI, Partridge IK. Cure modeling and monitoring of epoxy/amine resin system, I, cure kinetics modeling. *J Appl Polym Sci* 2000;77:1419–31.
- [13] Liu G, Zhang L. A new curing kinetic model and its application to BPSER/DDM epoxy system. *J Therm Anal Calorim* 2001;65:837–46.
- [14] Sun L, Pang S, Sterling A, Negulescu I, Stubblefield M, Stubblefield M. Thermal analysis of curing process of Epoxy Prepreg. *J Appl Polym Sci* 2002;83:1074–83.
- [15] Sun L, Pang S, Sterling A, Negulescu I, Stubblefield M. Dynamic modeling of curing process of Epoxy Prepreg. *J Appl Polym Sci* 2002;86:1911–23.
- [16] Moussa O, Vassilopoulos A, Keller T. Effects of low-temperature curing on physical behavior of cold-curing epoxy adhesives in bridge construction. *Int J Adhes Adhes* 2012;32:15–22.
- [17] Moussa O, Vassilopoulos A, Castro J, Keller T. Early-age tensile properties of structural epoxy adhesives subjected to low-temperature curing. *Int J Adhes Adhes* 2012;35:9–16.
- [18] Atarsia A, Boukhili R. Relationship between isothermal and dynamic cure of thermosets via the isoconversion representation. *Polym Eng Sci* 2000;40:607–20.
- [19] Chung TS. Cure mechanism of a modified nitrile epoxy adhesive. *J Appl Polym Sci* 1984;29:4403–6.
- [20] Li C, Zuo C, Fan H, Yu M, Li B. Novel silicone aliphatic amine curing agent for epoxy resin: 1,3-bis(2-aminoethylaminomethyl) tetramethyldisiloxane. 1. Non-isothermal cure and thermal decomposition property. *Thermochim Acta* 2012;545:75–81.
- [21] Chrissafis K, Roumeli E, Paraskevopoulos KM, Nianias N, Bikiaris DN. Effect of different nanoparticles on thermal decomposition of poly(propylene sebacate)/nanocomposites: evaluation of mechanisms using TGA and TG-FTIRGC/MS. *J Anal Appl Pyrolysis* 2012;96:92–9.
- [22] Papageorgiou GZ, Achilias DS, Karayannidis GP. Isoconversional glass transition kinetics and fragility determination of poly[(ethylene 2,6-naphthalate)-co-(butylene 2,6-naphthalate)] random copolymers. *Macromol Chem Phys* 2011;212:730–6.
- [23] Papageorgiou GZ, Achilias DS, Karayannidis GP. Estimation of thermal transitions in poly(ethylene naphthalate): experiments and modeling using isoconversional methods. *Polymer* 2010;51:2565–75.
- [24] Papageorgiou GZ, Achilias DS, Bikiaris DN. Crystallization kinetics of biodegradable poly(butylene succinate) under isothermal and non-isothermal conditions. *Macromol Chem Phys* 2007;208:1250–64.
- [25] Schawe JEK. A description of chemical and diffusion control in isothermal kinetics of cure kinetics. *Thermochim Acta* 2002;388:299–312.
- [26] Ristic MS, Pavlovic MG, Zlatar M, Blagojevic V, Andelkovic K, Poleti D, et al. Kinetics mechanism, and DFT calculations of thermal degradation of a Zn(II) complex with N-benzyloxycarbonylglycinato ligands. *Monatsh Chem* 2012;143:1133–9.
- [27] Achilias DS, Papageorgiou GZ, Karayannidis GP. Evaluation of the isoconversional approach to estimating the Hoffman–Lauritzen parameters from the overall rates of non-isothermal crystallization of polymers. *Macromol Chem Phys* 2005;206:1511–9.
- [28] Bosq N, Guigo N, Zhuravlev E, Sbirrazzuoli N. Non-isothermal crystallization of polytetrafluoroethylene in wide range of cooling rates. *J Phys Chem B* 2013;117:3407–15.
- [29] Sbirrazzuoli N. Determination of pre-exponential factors and of the mathematical functions  $f(\alpha)$  or  $C(\alpha)$  that describe the reaction mechanism in a model-free way. *Thermochim Acta* 2013;564:59–69.
- [30] Vyazovkin S, Dollimore D. Linear and nonlinear procedures in isoconversional computations of the activation energy of thermally induced reactions in solids. *J Chem Inf Comp Sci* 1996;36:42–5.
- [31] Vyazovkin S. Evaluation of the activation energy of thermally stimulated solidstate reactions under an arbitrary variation of the temperature. *J Comput Chem* 1997;18:393–402.
- [32] Vyazovkin S. Modification of the integral isoconversional method to account for variation in the activation energy. *J Comput Chem* 2001;22:178–83.
- [33] Chanda M, Rempel GL. Gel-coated ion-exchange resin: a new kinetic model. *Chem Eng Sci* 1999;54:3723–33.
- [34] Henne M, Breyer C, Niedermeier M. A new kinetic and viscosity model for liquid composite molding simulations in an industrial environment. *Polym Compos* 2004;25:255–69.
- [35] Lee CL, Wei KH. Curing kinetics and viscosity change of a two-part epoxy resin during mold filling in resin-transfer molding process. *J Appl Polym Sci* 2000;77:2139–48.
- [36] Gonis J, Simon GP, Cool WD. Application of isothermal and model-free isoconversional modes in DSC measurement for curing process of the PU system. *J Appl Polym Sci* 2001;81:1474–80.
- [37] Dusi MR, Galeos RM, Maximovich MG. Physiorheological characterization of a carbon/epoxy prepreg system. *J Appl Polym Sci* 1985;30:1847–57.
- [38] Morancho JM, Salla JM. Relaxation in partially cured samples of an epoxy resin and of the same resin modified with a carboxyl-terminated rubber. *Polymer* 1999;40:2821–8.
- [39] Vyazovkin S. In: Brown ME, Gallagher PK, editors. *The handbook of thermal analysis & calorimetry, recent advances, techniques and applications*, vol. 5. Amsterdam: Elsevier; 2008.
- [40] Arrhenius S. On the reaction rate of the inversion of non-refined sugar upon souring. *Z Phys Chem* 1889;4:226–48.
- [41] Yousefi A, Lafleur PG, Gauvin R. Kinetic studies of thermoset cure reactions: a review. *Polym Compos* 1997;18:157–68.
- [42] Málek J. The kinetic analysis of non-isothermal data. *Thermochim Acta* 1992;200:257–69.
- [43] Criado JM, Málek J, Ortega A. HTApplicability of the master plots in kinetic analysis of non-isothermal data. *Thermochim Acta* 1989;147:377–85.
- [44] Málek J. A computer program for kinetic analysis of non-isothermal thermo-analytical data. *Thermochim Acta* 1989;138:337–46.
- [45] Yang LF, Yao KD, Koh W. Kinetics analysis of the curing reaction of fast cure epoxy prepreps. *J Appl Polym Sci* 1999;73:1501–8.
- [46] Boey FYC, Qiang W. Experimental modeling of the cure kinetics of an epoxy-hexaamino-4-methylphthalic anhydride (MHHPA) system. *Polymer* 2000;41:2081–94.
- [47] Chan YC, Uddin MA, Alam MO, Chan HP. Curing kinetic of anisotropic conductive adhesive film. *J Electron Mater* 2003;32:131–6.
- [48] Vyazovkin S, Sbirrazzuoli N. Isoconversional kinetic analysis of thermally stimulated processes in polymers. *Macromol Rapid Commun* 2006;27:1515–32.
- [49] Sbirrazzuoli N. Is the Friedman method applicable to transformations with temperature dependent reaction heat? *Macromol Chem Phys* 2007;208:1592–7.
- [50] Doyle CD. Estimating isothermal life from thermogravimetric data. *J Appl Polym Sci* 1962;6:639–42.
- [51] Vyazovkin SV, Lesnikovich AI. Estimation of the pre-exponential factor in the isoconversional calculation of effective kinetic parameters. *Thermochim Acta* 1988;128:297–300.
- [52] Vyazovkin S, Linert W. The application of isoconversional methods for analyzing isokinetic relationships occurring at thermal decomposition of solids. *J Solid State Chem* 1995;114:392–8.
- [53] Vyazovkin S, Linert W. Thermally induced reactions of solids: isokinetic relationships of non-isothermal systems. *Int Rev Phys Chem* 1995;14:355–69.
- [54] Budrugaec P, Segal E, Pérez-Maqueda LA, Criado JM. The use of the IKP method for evaluating the kinetic parameters and the conversion function of the thermal dehydrochlorination of PVC from non-isothermal data. *Polym Degrad Stab* 2004;84:311–20.
- [55] Cadenato A, Morancho JM, Fernández-Francos X, Salla JM, Ramis X. Comparative kinetic study of the non-isothermal thermal curing of bis-GMA/TEGDMA systems. *J Therm Anal Calorim* 2007;89:233–44.
- [56] Kamal MR. Thermoset characterization for moldability analysis. *Polym Eng Sci* 1974;14:231–9.
- [57] Kamal MR, Sourour S. Kinetic and thermal characterization of thermoset cure. *Polym Eng Sci* 1973;13:59–64.
- [58] Chan AW, Hwang ST. Modeling of the impregnation process during resin transfer molding. *Polym Eng Sci* 1991;31:1149–56.
- [59] Gebart BR. Critical parameters for heat transfer and chemical reactions in thermosetting materials. *J Appl Polym* 1994;51:153–68.
- [60] Keenan MR. Autocatalytic cure kinetics from DSC measurements: zero initial cure rates. *J Appl Polym* 1987;33:1725–34.
- [61] Riccardi CC, Adabbo HE, Williams RJ. Cure mechanism of a modified nitrile epoxy adhesive. *J Appl Polym* 1984;29:4403–6.